In Situ Sol-Gel Process of Polystyrene/Silica Hybrid Materials: Effect of Silane-Coupling Agents

JYONGSIK JANG, HWANSEOK PARK

Hyperstructured Organic Materials Research Center, School of Chemical Engineering, Seoul National University, San 56-1, Shinlimdong, Kwanakgu, Seoul, Korea

Received 24 April 2001; accepted 14 November 2001

ABSTRACT: The polystyrene–silica hybrid materials have been successfully prepared from styrene and tetraethoxysilane in the presence of silane-coupling agents by an *in situ* sol-gel process. Triethoxysilyl group can be incorporated into polystyrene as side chains by the free-radical copolymerization of polystyrene with silane-coupling agents, and simultaneously polystyrene–silica hybrid materials with covalent bonds between two phases were formed via the sol-gel reaction. The 3-(trimethoxysilyl)-propyl-methacrylate (MPS) systems were found to be more homogeneous than the corresponding allytrimethoxysilane hybrid system of equal molar content. In the MPS-introduced system, the thermal properties of the materials were greatly affected by the presence of MPS. FTIR results indicate successful formation of the silica networks and covalent bonding formation of coupling agents with styrene. The homogeneity of polystyrene–silica systems was examined by scanning electron microscope and atomic force microscope. © 2002 Wiley Periodicals, Inc. J Appl Polym Sci 85: 2074–2083, 2002

INTRODUCTION

The sol-gel chemistry is based on the polymerization of inorganic precursors such as metal alkoxides. The reaction is divided into two steps. Hydrolysis and condensation of metal alkoxides led to the formation of inorganic network.[1,2] Recently, the sol-gel reaction was used to prepare the organic–inorganic hybrid materials.[3–5] The properties of a composite material depend not only on the properties of each component, but also on the composite's phase morphology and interfacial properties. Thus, morphology and phase separation controls are important in the preparation of organic–inorganic composites. On the basis of the interfacial interaction between the organic and the inorganic phases, the organic–inorganic hybrid materials can be classified into two distinct types. The first type is due to formation of the extensive hydrogen bonding between the hybrid materials, and the second type is connected to each other by covalent bonds. Various polymers, such as poly(methyl methacrylate),[6,7] poly(vinyl acetate),[8,9] poly(vinyl pyrrolidone),[10] poly(dimethylsiloxane),[11,12] epoxy,[13] and polyimides,[14,15] were successfully incorporated into inorganic networks by the sol-gel process, and these hybrid materials can exhibit excellent optical transparency.

In general, the coupling agents were utilized to introduce chemical bond between organic and inorganic phases.[16] In the conventional composite systems, coupling agents may function as a finish or surface modifier, a primer or size, or as an adhesive, depending on the thickness of the bonding material at the interface. Although coupling agents may perform several useful functions at the interface in composite systems, the coupling agent is expected, first of all, to improve the adhesion between organic and inorganic components and improve retention of properties under a variety of circumstances.

Correspondence to: J. Jang (jsjang@plaza.snu.ac.kr).
Contract grant sponsor: RIES.

Journal of Applied Polymer Science, Vol. 85, 2074–2083 (2002)

Table I Compositions and Thermal Properties of the Prepared Hybrids

		Feed Ratio			SiO_2 (wt %)		
Sample	SCA	ST : TEOS (w/w)	SCA : TEOS (mol/mol)	T_g (°C)[a]	Ther.[b]	Exp.[c]	DTG (°C)[d]
EMPS	MPS	2:1	1:2	114.33	15.78	15.58	388.08
EALS	ALS	2:1	1:2	74.89	17.06	25.20	410.86
ENO	—	2:1	—	67.70	12.59	13.47	411.81
ES1	MPS	1:1	1:1	—	26.33	32.08	395.03
ES6	MPS	6:1	1:1	98.50	8.01	14.32	406.51
ES20	MPS	20:1	1:1	86.60	2.72	4.94	422.99
EM01	MPS	2:1	0.1:1	96..39	12.11	12.63	370.34
EM1	MPS	2:1	1:1	113..65	18.07	19.12	385.41
EM2	MPS	2:1	2:1	110.59	21.74	29.74	409.40

[a] Determined by DSC.
[b] Assuming full condensation of TEOS.
[c] Calculated from TGA.
[d] Main peak of the 1st derivative.

In numerous research, silane-coupling agents were used for reducing the phase separation at the interface between organic and inorganic phases. Polystyrene (PS) and styrene (St) copolymers were successfully incorporated with inorganic parts by different synthetic methods.[17–20] The introduction of alkoxy silyl group into organic polymer chain by the copolymerization makes it possible to control the phase separation. Although this method is effective, the copolymers containing trialkoxysilane have some problem to be handled because these types of copolymers are hydrolytically unstable.

The purpose of this work was to study the effect of the silane-coupling agents on the thermal and morphological properties of PS–silica hybrid materials. PS–silica hybrid materials were prepared by the *in situ* synthesis of the silica phase during the free-radical polymerization of styrene in the presence of silane-coupling agents. The rate and degree of conversion from vinyl monomer to polymer may significantly influence the properties of these hybrid materials as well as the selection of the appropriate silane-coupling agents to enhance the properties. The influence of the rate of polymerization on the structure and morphology of organic–inorganic hybrid materials was previously demonstrated for interpenetrating polymer networks of silica and acrylate polymers.[21]

In the present work, the relationships between the degree of conversion of vinyl group and the properties of hybrid materials were studied. In addition, the effect of the ratio of individual components on the properties of hybrid materials was undertaken. The hybrid materials were characterized with Fourier transform infrared spectroscopy (FTIR), differential scanning calorimeter (DSC), thermogravimetric analysis (TGA), and atomic force microscopy (AFM).

EXPERIMENTAL

Materials

Tetraethoxysilane (TEOS, Merck) was used as received. Styrene (St, Junsei) was washed with 5% NaOH aqueous solution to remove inhibitors and distilled under reduced pressure. 3-(Trimethoxysilyl)-propyl-methacrylate (MPS, Aldrich) and allytrimethoxysilane (ALS, Aldrich) were purified by distillation under vacuum. 2,2′-Azobisisobutyronitrile (AIBN, Aldrich) was recrystallized from methanol. AIBN was used as a free-radical initiator and 1*M* HCl and tetrahydrofuran (THF, Daejung Chemical, Korea) were used as catalyst and solvent, respectively.

Preparation of the PS–Silica Hybrid Materials

Polymer–silica hybrid materials were prepared by undergoing free-radical copolymerization of St with silane-coupling agents (i.e., MPS, ALS) during the simultaneous *in situ* growing of the silica phase through the acid-catalyzed sol-gel reaction of TEOS. All samples are listed in Table I and the synthetic route is shown in Figure 1. An appropriate amount of TEOS, silane-coupling agents, and 1*M* HCl were dissolved in THF. After the

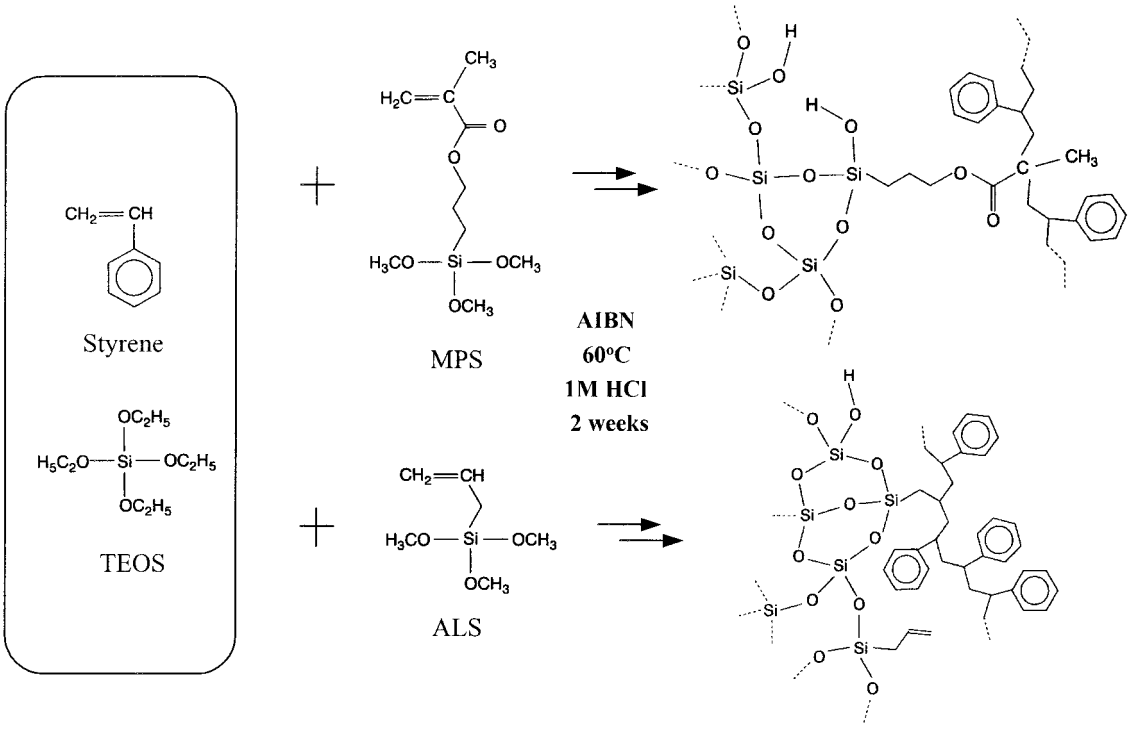

Figure 1 Preparation scheme of PS-SiO_2 hybrid materials.

mixture was stirred for 1 h, St and AIBN were poured directly into the solution under continuous agitation. Then, the samples were allowed to stand at 60°C for 2 weeks.

Measurement

FTIR spectra were obtained in the transmission mode between 400 and 4000 cm^{-1} by using the Bomem MB 100 with a 4 cm^{-1} resolution. Samples were prepared by casting the precursor solution on KBr pellets which are pressed by KBr powder. TGA was performed on a Perkin–Elmer TGA7 with a heating rate of 10°C/min under air condition. DSC data were obtained from TA2100 in the temperature range 25–200°C. All samples were tested at a heating rate of 10°C/min under nitrogen flow. SEM measurement was conducted by using the JSM840-A model. AFM images were taken with the Digital Instruments Nanoscope IIIa atomic force microscope in contact mode with the silicon nitride (Si_3N_4) probe tips. AFM measurements were performed on the fresh fracture surfaces prior to scanning.

RESULTS AND DISCUSSION

Effect of Silane-Coupling Agents

The PS–silica hybrid materials were synthesized via simultaneous polymerization of St and TEOS in the presence of MPS and ALS, respectively. The procedure is schematically described in Figure 1.

Figure 2 gives FTIR spectra for the (a) PS-MPS-silica (EMPS), (b) PS-ALS-silica (EALS), and (c) no coupling agents contained PS-silica (ENO) samples. These three spectra display 1600–1575 and 690 cm^{-1} absorption peaks related to the aromatic ring of PS, and 1220, 1080, 800, and 460 cm^{-1} absorption peaks associated with Si—O—Si linkages. A comparison shows that the characteristic absorption peak for C═C of the units from ALS appears at 1634 cm^{-1}. This indicates that ALS was not perfectly copolymerized with St during the *in situ* sol-gel process. For quantitative analysis, the 690 cm^{-1} peak, which was related to out-of-plane ring deformation of a monosubstituted phenyl group, is employed as internal reference peak.[22] In the case of EALS, the conversion of ALS was calculated as follows:

$$\text{Conversion (\%)} = \frac{[\text{C═C peak area of the precursor}] - [\text{C═C peak area of the hybrid}]}{[\text{C═C peak area of the precursor}]} \times 100$$

The conversion value of ALS was about 41%. For the MPS, however, C═C peak is not observed in Figure 2(a). These results show that the reactivity of ALS with St is lower than that of MPS. This

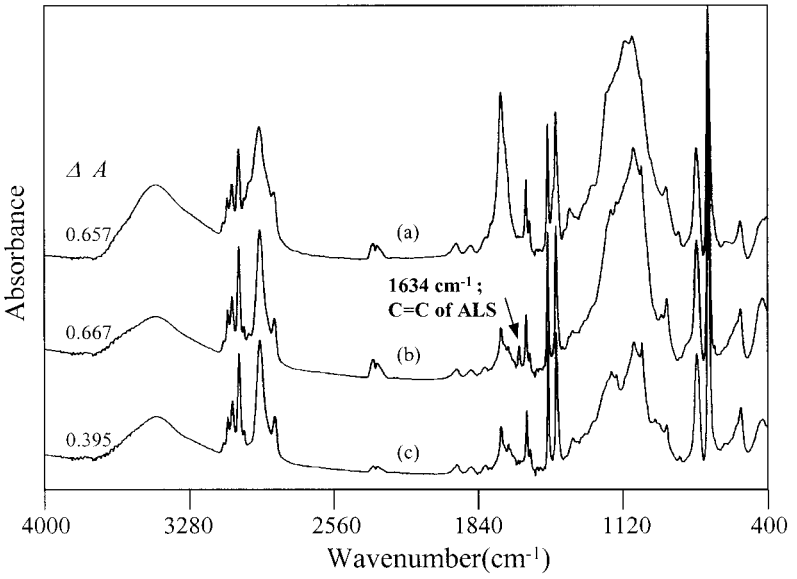

Figure 2 FTIR spectra of (a) EMPS, (b) EALS, and (c) ENO.

may be due to autoinhibition of allylic groups.[23] Generally, the allylic radicals are too stable to initiate polymerization and the kinetic chain also terminates when the transfer occurs. Additionally, the chain mobility of MPS fixed to the silica network through sol-gel reaction is more active than that of ALS, and ALS is easily entrapped to the silica network due to molecular size. Thus, MPS has the possibility of reacting with the propagating center.

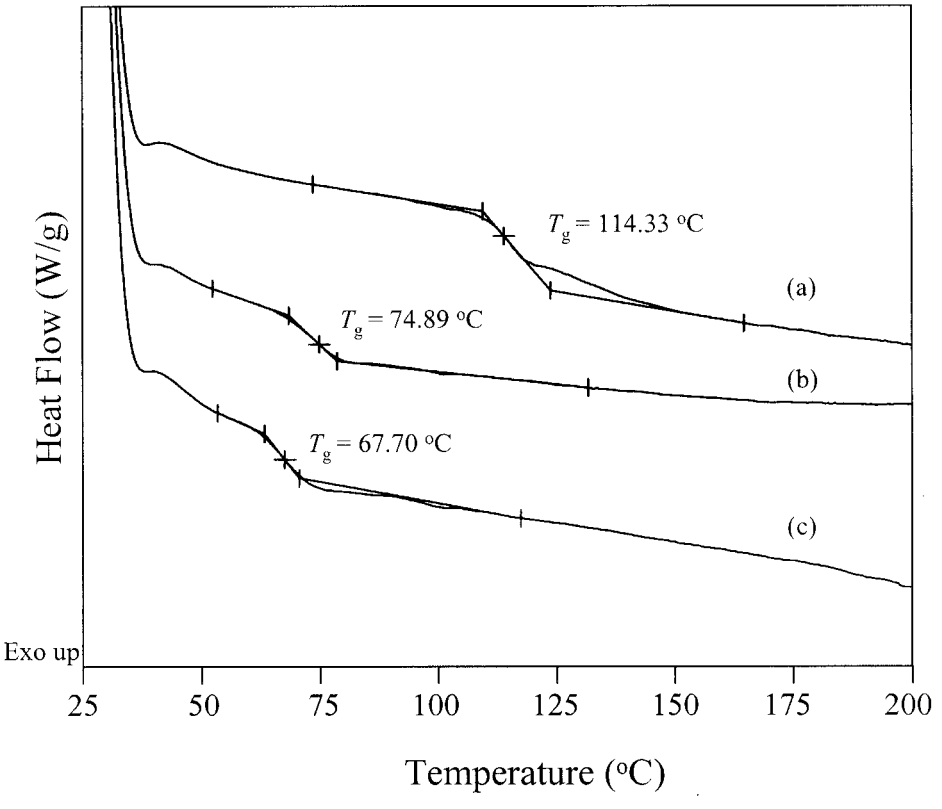

Figure 3 DSC thermograms of (a) EMPS, (b) EALS, and (c) ENO.

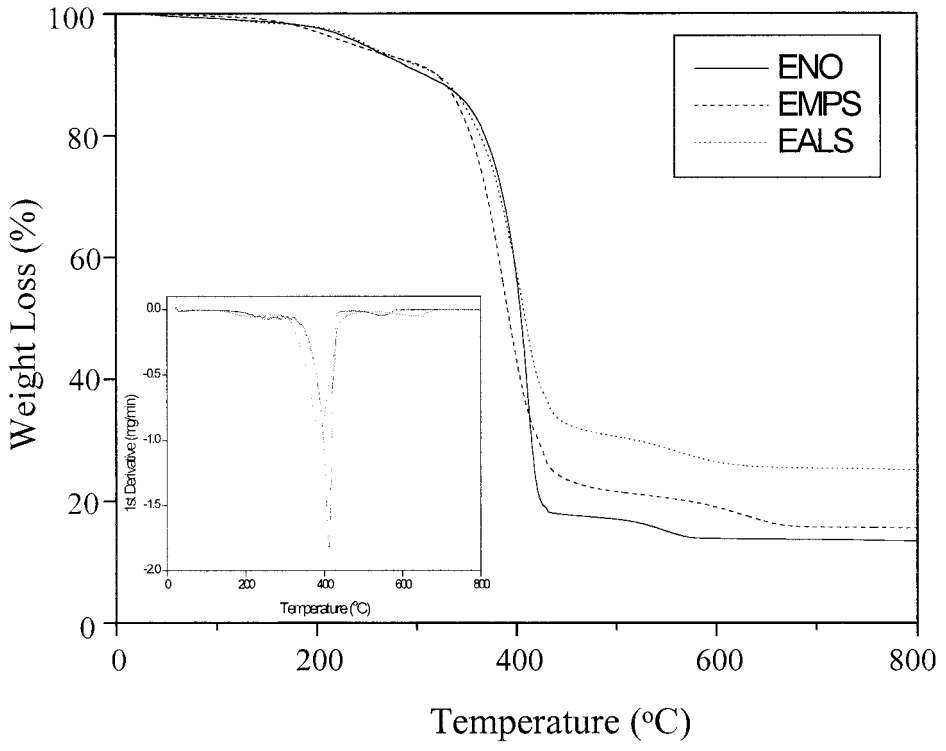

Figure 4 TGA and DTG thermograms of the hybrid materials.

The glass transition temperature (T_g) behavior of the hybrid materials is associated with not only each component but also the nature of the interface between the two components. The DSC results of (a) EMPS, (b) EALS, and (c) ENO samples, shown in Figure 3, reveal shifts in the T_g of PS in the hybrid materials. Apparently, the T_g of EMPS progressively shifts to higher values than

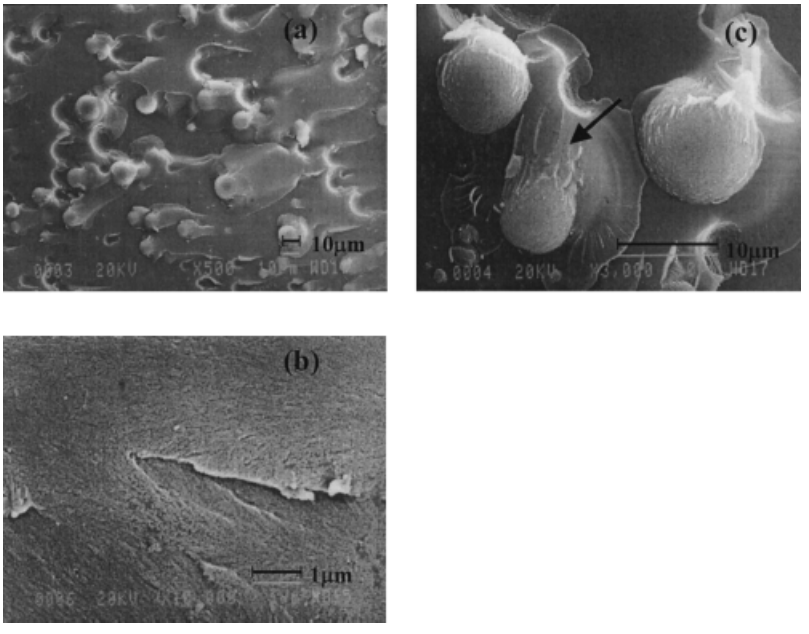

Figure 5 SEM micrographs of (a) EALS, (b) EMPS, and (c) magnified micrograph of (a).

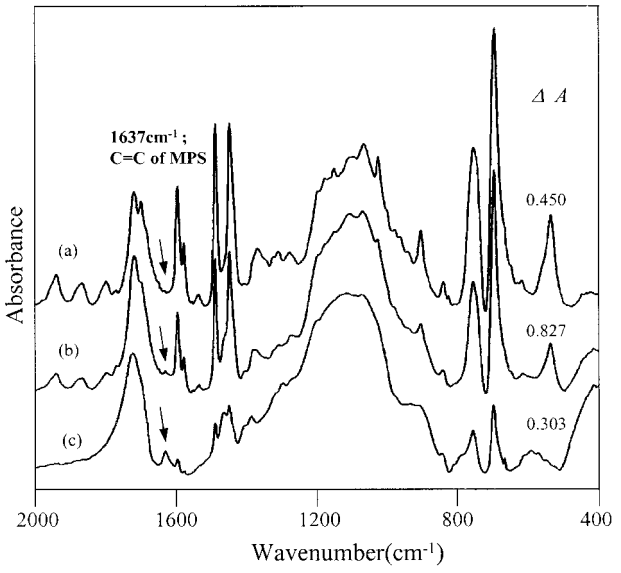

Figure 6 FTIR spectra of (a) ES20, (b) ES6, and (c) ES1.

ENO, whereas the T_g of EALS increases only slightly. The results suggest increased adhesion between the two phases, the polymer and the silica. The considerable shifts in T_g values are obviously the reason for the improved bonding. On this basis, there are strong interfacial interactions between the polymer chains and the silica phase with the addition of coupling agents.

Figure 4 shows the TGA and DTG thermograms of the hybrid materials. The thermal stabilities of the samples may be influenced by silane-coupling agents. The thermal degradation behavior of EALS is similar to that of ENO, but the thermal stability of EMPS deteriorates when MPS is introduced to the interface. From DTG results, we can obtain the temperature of the maximum rate of loss of weight ($T_{d,\max}$). Because the thermal degradation of the EMPS is initially caused by the decomposition of methacrylate, $T_{d,\max}$, as shown DTG, is lower than those of ENO and EALS.

The evidence for covalent bond formation at the interface between silane-coupling agents (i.e., MPS, ALS) and PS matrix was already obtained from IR and DSC results. Although the chemical bonds exist in the hybrid systems, the macroscopic phase separation still takes place in the EALS. Microscale particles can clearly be observed in Figure 5(a). However, it can be also observed that there is homogeneous region due to

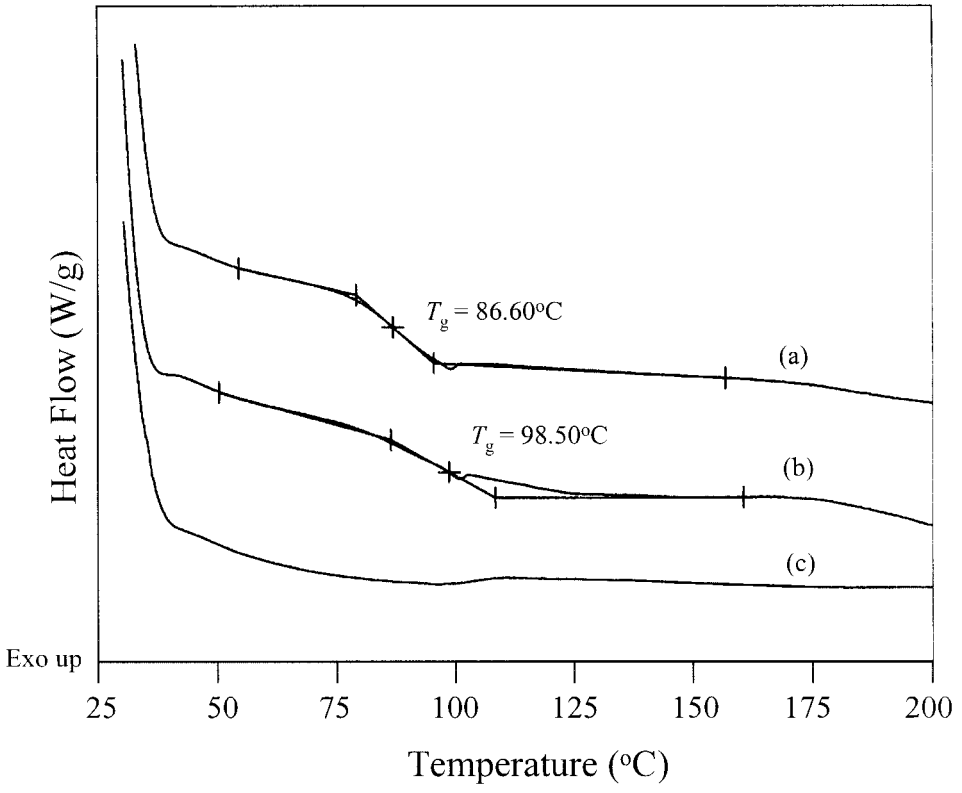

Figure 7 DSC thermograms of (a) ES20, (b) ES6, and (c) ES1.

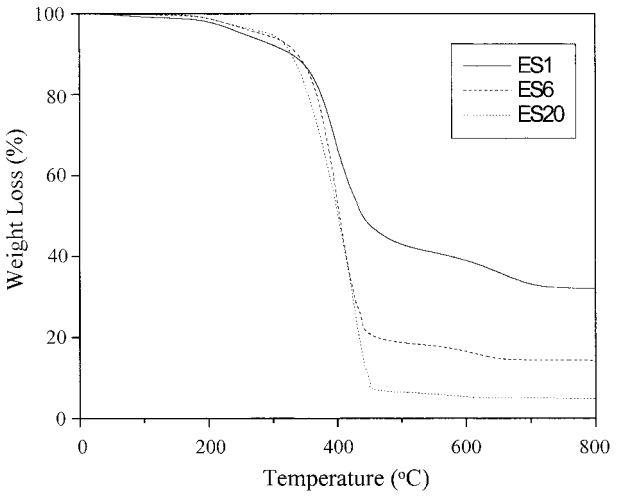

Figure 8 TGA thermograms of the hybrid materials.

interfacial constraint between silica particle and polymer matrix, as shown in Figure 5(c). Even if ALS has low reactivity with St, this is obviously due to the adhesion of the interface between two phases. For EMPS [Fig. 5(b)], there is no macrophase separation for the hybrid materials (i.e., EMPS).

The result illustrates the effect of using silane-coupling agents for improving the properties of hybrid materials. Although MPS negatively affects the thermal stability, MPS is effective to restrict the phase separation because of its high reactivity to the styrene monomer.

Effect of St Contents

Figure 6 shows the FTIR spectra of the hybrid materials, (a) ES20, (b) ES6, and (c) ES1. In the FTIR spectra, the influence of St contents on the copolymerization of St and MPS was clearly illustrated. As the St contents increase, the C═C absorption band of MPS (1637 cm^{-1}) disappears. At the low styrene contents, the free-radical copolymerization may be restricted by the gelation of TEOS. The silica networks reduce the molecular motion of the St. Additionally, although unreacted MPS still remains in the samples, all the samples obtained in the presence of MPS are transparent.

The measurements of the T_g were used to determine the miscibility of polymer blends.[24] This is based on the premise that a single T_g indicates that the domain size is below 15 nm. The detection of a single T_g, whose value is shifted to the intermediate between the values of the component polymers, is an indication of no phase separation. The DSC results presented in Figure 7 show the T_g's of (a) ES20, (b) ES6, and (c) ES1. When the weight ratio of St to TEOS is high, the hybrids have a nearly coincident T_g (67.70°C) value of PS. As the St contents decrease, the T_g of the hybrids increases and consequently cannot be detected. Such a behavior of T_g was attributed to the confinement of the PS molecular chain, and the quantity of confinement may be determined by the relative ratio of PS and TEOS at the same content of MPS. This result is similar to the T_g behavior of the miscible blends (i.e., the T_g of a miscible blend is highly dependent on the composition of the system).

The heat resistance of polymer may be characterized by its temperature of initial and of half decomposition.[25] Figure 8 illustrates TGA thermograms for ES1, ES6, and ES20. At the 5% weight loss, the prepared hybrids have thermal

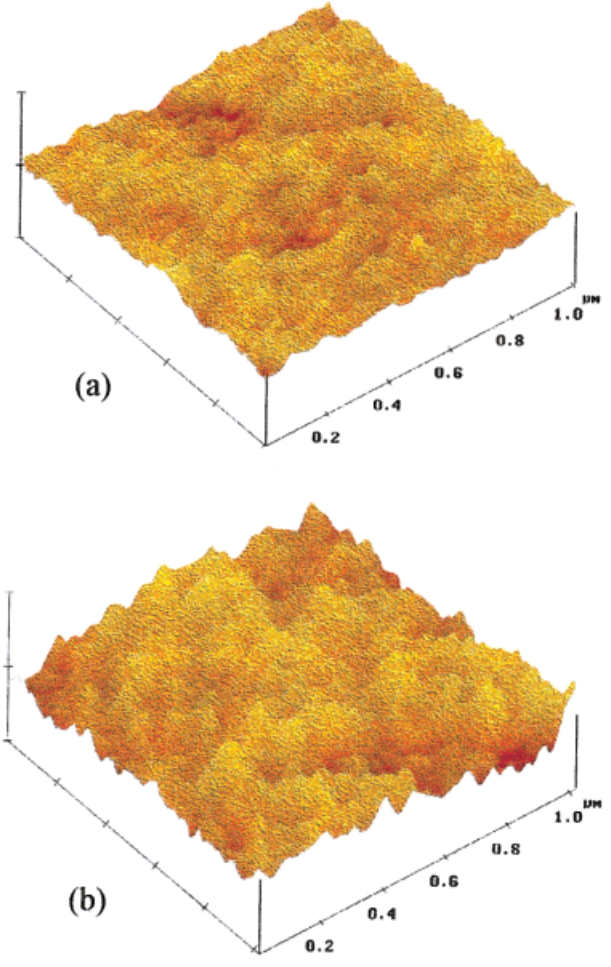

Figure 9 AFM images of (a) ES1 and (b) ES20; Z range is 70 nm. [Color figure can be viewed in the online issue, which is available at www.interscience.wiley.com.]

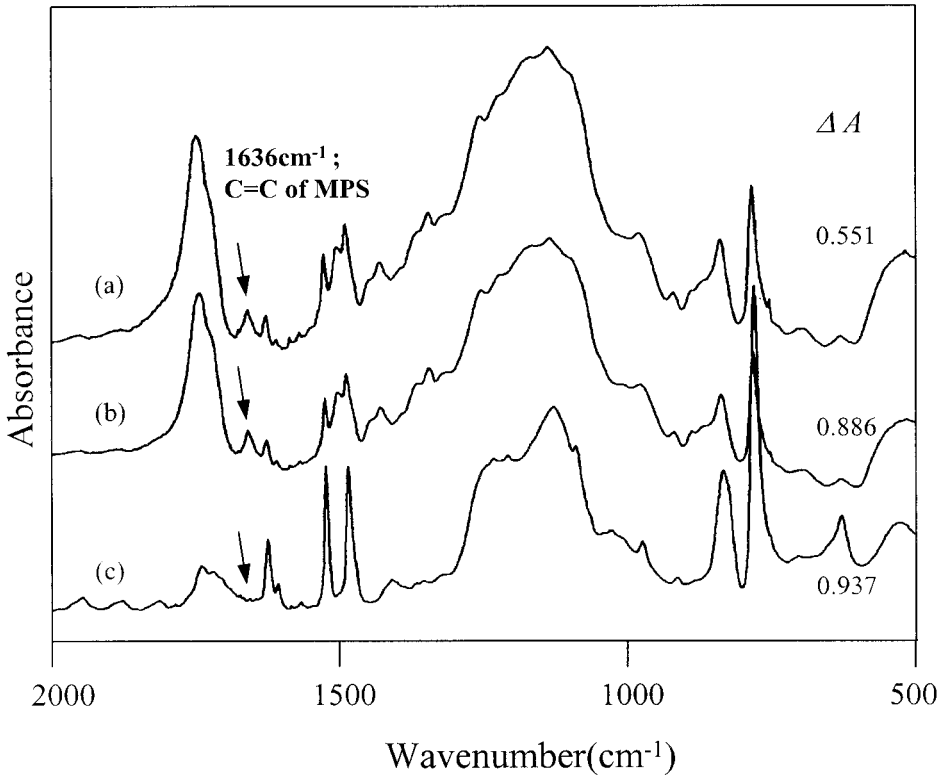

Figure 10 FTIR spectra of (a) EM2, (b) EM1, and (c) EM01.

decomposition temperatures of 255.7, 284.1, and 297.1°C for ES1, ES6, and ES20, respectively. This is probably due to destruction of the MPS because of the low-bond dissociation energy of the methacrylate group. Also, the $T_{d,\max}$'s obtained from DTG show this tendency. However, at the 50% weight loss ($T_{d,1/2}$), ES20 has the lowest value (400.8°C) and ES1 has the highest value (439.4°C). In this case, $T_{d,1/2}$ may be affected by the ratio of St to TEOS. The above results suggest using a higher content of St (i.e., low content of methacrylate group) and a higher content of inorganic moiety to relatively enhance the thermal stability.

Figure 9 shows two representative topographic views of the samples. At a low St content [Fig. 9(a)], the transparent sample exhibits relatively smooth and random fracture surface, showing no particular topographic contrast. Although the image of ES20 is rougher, the appearance of the two samples is very similar. The mean roughness values of the hybrid ES1 and ES20 are 30.64 and 79.59 Å, respectively. In general, the modulus of the hybrids increase significantly with increasing silica content,[26] and thus the hybrids become very brittle. At a high silica content [Fig. 9(a)], the sample should reveal a much finer fracture surface.

Effect of MPS Contents

Figure 10 gives the FTIR spectra of (a) EM2, (b) EM1, and (c) EM01. These spectra display a broad band between 1000 and 1200 cm^{-1} related to the presence of Si—O—Si group from SiO_2 network and their intensities increase with increasing MPS contents. The relatively strong C═C stretching band of MPS is shown in Figure 10(a,b). The degree of conversion of MPS can be determined by using the same method previously described. Interestingly, both (a) EM2 and (b) EM1 have a similar degree of conversion, that is, about 80%. In the spectrum (c), no band consistent with C═C stretching vibration of MPS appears. As the MPS contents increase, the amount of unreacted MPS also increases until the saturation point. In other words, increasing MPS concentration is not a good solution to be introduced into a chemical bond between organic and inorganic parts. Considering the results of DSC (Fig. 11), the above conclusion is the basis of a certain amount of MPS; beyond this amount of MPS, we can get the above conclusion.

The DSC results of EM01, EM1, and EM2 samples, as shown in Figure 11, reveal an increase in the onset of the glass transition of PS in the composite and a similar T_g for EM1 and EM2. If

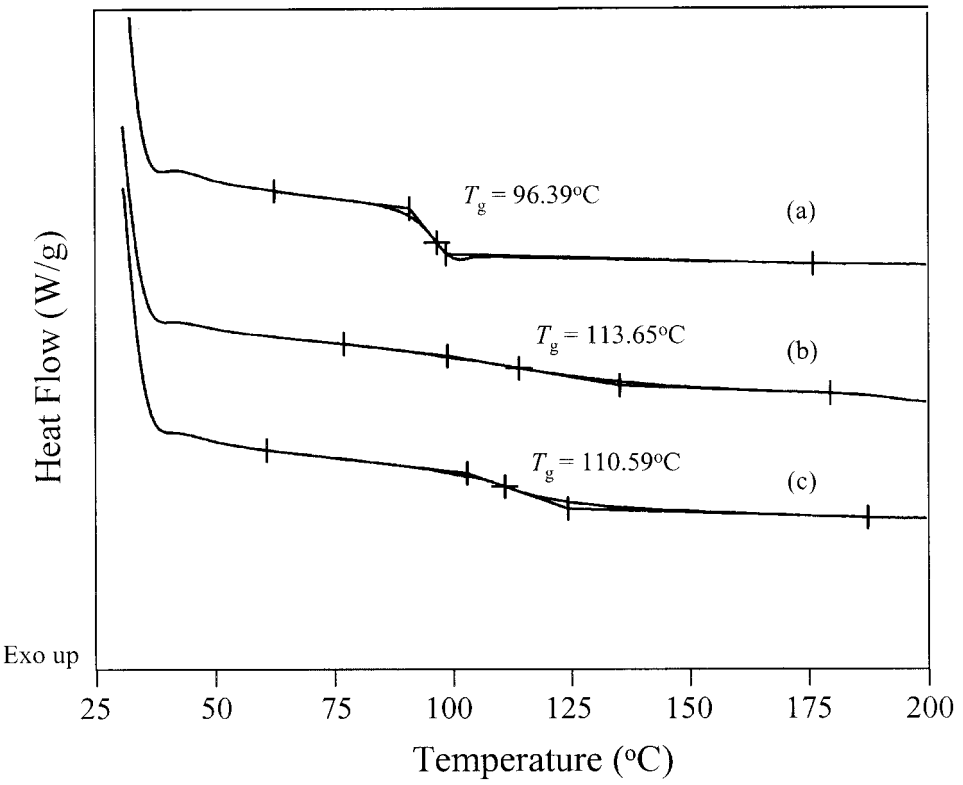

Figure 11 DSC thermograms of (a) EM01, (b) EM1, and (c) EM2.

the content of coupling agents is high enough, the increasing of T_g with an increase of the inorganic component content can be observed.

As previously discussed, the thermal degradation of the hybrids containing MPS is mainly influenced by the cleavage of methacrylate. However, Figure 12 shows that the thermal decomposition of the hybrid could be affected by another factor. In EM series, the samples would become higher, crosslinking with increasing the contents of MPS, and consequently this effect may be more critical than the decomposition of the methacrylate. The results of the DTG (Table I) of the EM series also show that thermal stability is enhanced by increasing MPS content.

Representative AFM images of the hybrids are illustrated in Figure 13. Figure 13(a) shows a height image, while Figure 13(b) is the friction image obtained at the same time. Because the friction force is higher on the silica surface than on the PS, the difference of the contrast should occur in the two component systems. The height image has two regions (i.e., dark and bright), but the friction image does not show the obvious difference of the contrast. This implies that the contrast of height image is only due to the topographical features of the fracture surfaces. Thus, we are convinced that there was no macrophase separation between organic and inorganic phases.

CONCLUSION

PS-SiO_2 hybrid materials with chemical bonds between organic and inorganic phases were pre-

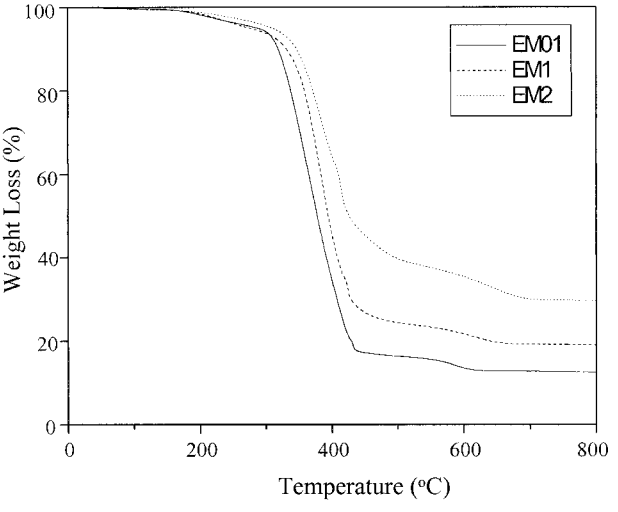

Figure 12 TGA thermograms of the hybrid materials.

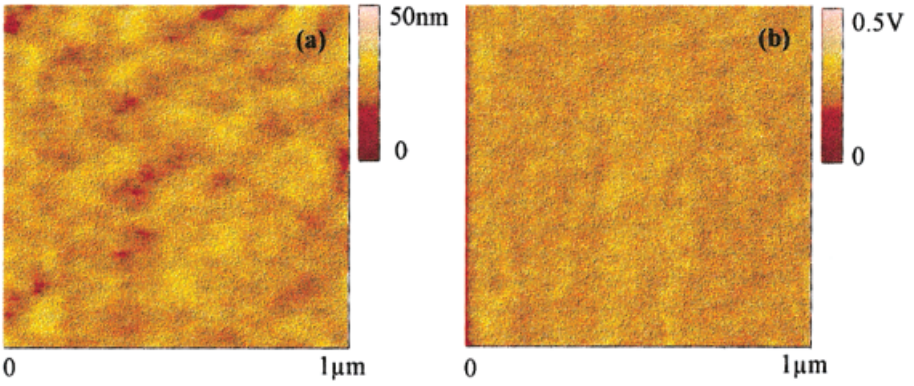

Figure 13 AFM images of EM01 (a) height image and (b) friction image, which show that there is no phase separation between organic and inorganic components. [Color figure can be viewed in the online issue, which is available at www.interscience.wiley.com.]

pared by *in situ* sol-gel method. It was shown that the reactivity of MPS with St was higher than that of ALS, and the hybrid materials prepared by introducing silane-coupling agents, especially MPS, acquired better homogeneity. The presence of the silane-coupling agents caused increases in T_g due to the molecular motions of the organic polymer being restricted by the inorganic phases. The thermal degradation behavior of materials was extremely affected by the silane-coupling agents. With the use of different contents of coupling agents, the hybrids would show different thermal decomposition properties due to the variation in the portion of crosslinking in the hybrid systems. From the results above, we conclude that the appropriate amount and kind of coupling agent should be determined by their reactivity with organic components.

The authors gratefully acknowledge the research support of Research Institute of Engineering Science (RIES).

REFERENCES

1. Hench, L. L.; West, J. K. Chem Rev 1990, 90, 33.
2. Brinker, C. J.; Scherer, G. W. Sol-Gel Science: The Physics and Chemistry of Sol-Gel Processing; Academic Press: New York, 1990.
3. Novak, B. M. Adv Mater 1993, 5, 422.
4. Wen, J.; Wilkes, G. L. Chem Mater 1996, 8, 1667.
5. Sanchez, C.; Ribot, F.; Lebeau, B. J Mater Chem 1999, 9, 35.
6. Chen, W.; Lee, S.; Lee, L.; Lin, J. J Mater Chem 1999, 9, 2999.
7. Pu, Z.; Mark, J. E.; Jethmalani, J. M.; Ford, W. T. Chem Mater 1997, 9, 2442.
8. Fitzgerald, J. J.; Landry, C. J. T.; Pochan, J. M. Macromolecules 1992, 25, 3715.
9. Landry, C. J. T., Coltrain, B. K.; Landry, M. R.; Fitzgerald, J. J.; Long, V. K. Macromolecules 1993, 26, 3702.
10. Toki, M.; Chow, T. Y.; Ohnaka, Y.; Samura, H.; Saegusa, T. Polym Bull 1992, 29, 653.
11. Sun, C.-C.; Mark, J. E. Polymer 1989, 30, 104.
12. Yuan, Q. W.; Mark, J. E. Macromol Chem Phys 1999, 200, 206.
13. Mascia, L.; Tang, T. J Mater Chem 1998, 8 (11), 2417.
14. Kioul, A.; Mascia, L. J Non-Cryst Solids 1994, 175, 169.
15. Wu, K. H.; Chung, T. C.; Wang, Y. T.; Chiu, Y. S. J PolymSci, Part A: Polym Chem 1999, 37, 2275.
16. Plueddemann, E. P. Silane Coupling Agents; Plenum: New York, 1982.
17. Hsiue, G. H.; Kuo, W. J.; Huang, Y. P.; Jeng, R. J. Polymer 2000, 41, 2813.
18. Tamaki, R.; Chujo, Y. Chem Mater 1999, 11, 1719.
19. Tamaki, R.; Samura, K.; Chujo, Y. Chem Commun 1998, 10, 1131.
20. Ikeda, Y.; Tanaka, A.; Kohjiya, S. J Mater Chem 1997, 7 (8), 1497.
21. Jackson, C. L.; Bauer, B. J.; Nakatani, A. I.; Barnes, J. D. Chem Mater 1996, 8, 727.
22. Colthup, N. B.; Daly, L. H.; Wiberley, S. E. Introduction to Infrared and Raman Spectroscopy; Academic Press: New York, 1975.
23. Odian, G. Principles of Polymerization, 3rd ed.; Wiley: New York, 1991.
24. Utracki, L. A. Polymer Alloys and Blends; Hanser: New York, 1989.
25. Van Krevelen, W. Properties of Polymers, 3rd ed.; Elsevier: Amsterdam, 1990.
26. Yano, S.; Iwata, K.; Kurita, K. Mater Sci Eng, C 1998, 6, 75.